Performances of One-Dimensional Sonomyography and Surface Electromyography in Tracking Guided Patterns of Wrist Extension

Jing-Yi Guo[1], Yong-Ping Zheng[1,2], Qing-Hua Huang[1], Xin Chen[1], Jun-Feng He[1], Helen Lai-Wa Chan[3]

[1] Department of Heath Technology and Informatics, [2] Research Institute of Innovative Products and Technologies, [3] Department of Applied Physics, The Hong Kong Polytechnic University, Kowloon, Hong Kong, China

Corresponding author:

Dr. Yongping Zheng

Address: Department of Heath Technology and Informatics
The Hong Kong Polytechnic University
Kowloon, Hong Kong SAR, China

Tel: +852 27667664

Fax: +852 23624365

Email: ypzheng@ieee.org

Abstract

Electromyography (EMG) and ultrasonography have been widely used for skeletal muscle assessment. Recently, it has been demonstrated that the muscle thickness change collected by ultrasound during contraction, namely sonomyography (SMG), can also be used for assessment of muscles and has the potential for prosthetic control. In this study, the performances of one-dimensional sonomyography (1-D SMG) and surface EMG (SEMG) signal in tracking the guided patterns of wrist extension were evaluated and compared, and the potential of 1-D SMG for skeletal muscle assessment and prosthetic control was investigated. Sixteen adult normal subjects including eight males and eight females participated in the experiment. The subject was instructed to perform the wrist extension under the guidance of displayed sinusoidal, square and triangular waveforms at movement rates of 20, 30, 50 cycles per minute. SMG and SEMG root mean squares (RMS) were collected from the extensor carpi radialis respectively and their RMS errors in relation to the guiding signals were calculated and compared. It was found that the mean RMS tracking errors of SMG under different movement rates were 18.9±2.6% (mean± SD), 18.3±4.5%, and 17.0±3.4% for sinusoidal, square, and triangular guiding waveforms, while the corresponding values for SEMG were 30.3±0.4 %, 29.0±2.7%, and 24.7±0.7 %, respectively. Paired t-test showed that the RMS errors of SMG tracking were significantly smaller than those of SEMG. Significant differences in RMS tracking errors of SMG among the three movement rates ($p<0.01$) for all the guiding waveforms were also observed using one-way ANOVA. The results suggest that SMG signal, based on further improvement, has great potential to be an alternative method to SEMG to evaluate muscle function and control prostheses.

Keywords- ultrasound, sonomyography, SMG, electromyography, EMG, muscle, prosthetic control

INTRODUCTION

Both electromyography (EMG) and ultrasonography have been widely used to detect the skeletal muscle properties and movements during static and dynamic contractions. EMG describes the bioelectrical properties of skeletal muscles and reveals the physiological process of the muscle contraction. It is generated by the irregular discharges of active motor unit (MU) during the muscle activation (Zwarts and Stegeman 2003). The root mean square (RMS) magnitude of EMG is commonly used to describe the time-domain information of EMG signal (Karlsson and Gerdle 2001). However, despite its wide applications in different areas, EMG has some inherent limitations. It is difficult for surface EMG to detect the deep muscles non-invasively, due to the fact that the deep muscle EMG may be attenuated more and mixed by the superficial muscle EMG when reaching the skin surface. EMG signals could vary seriously from people to people even performing the same task (Balogh et al. 1999) and be influenced by many factors, such as muscle cross talk (De Luca 2002), and interelectrode distance (Alemu et al. 2003). In addition, commercially available upper-limb externally powered prosthetic devices using EMG are still limited to one or few degrees of freedom (DoFs) (Zecca et al. 2002). On the other hand, some alternative approaches have been investigated to generate signals for control purposes, including surface electroencephalography (EEG) (Heasman et al. 2002), collected using embedded neurochip implants (Nicolelis 2001; Taylor et al. 2002); acoustic signals generated by muscles (Oster 1984; Bolton et al. 1989; Orizio et al. 1993), muscle dimensional change (Almstrom and Kadefors 1972; Kenny et al. 1999), and tendon motions (Abboudi et al. 1999; Curcie et al. 2001), etc. These methods each have their own advantages and shortcomings and researchers in this field are still working hard to achieve signals for a better prosthetic control, such as to reduce the cognitive effort required of users, to provide direct feedback when performing movement, and to increase the number of degrees of freedom (DoFs).

Ultrasonography is another widely used method to measure muscle morphology change and it has been used together with EMG to provide more comprehensive information about the muscle activities and properties (Whittaker et al., 2007). Researchers using ultrasound images have successfully detected the changes of muscle thickness (Sallinen et al. 2008), pennation angle (Mahlfeld et al. 2004), cross-sectional areas (Reeves et al. 2004) and muscle fascicle length (Fukunaga et al. 2001) in both static and dynamic conditions. Since skeletal muscle architecture is closely correlated with its function (Lieber and Friden 2000), the ultrasound parameters have been employed to characterize muscle activities (Maganaris et al. 2001; Mademli and Arampatzis 2005). In addition, it has been reported that the relationship between EMG and the muscle morphological changes extracted from ultrasound is almost linear only in lower range of forces, but not in higher range of forces for tibialis anterior (Hodges et al. 2003), biceps brachii (Hodges et al. 2003; Shi et al. 2008), transversus abdominis (Hodges et al. 2003; McMeeken et al. 2004), masseter muscle (Georgiakaki et al. 2007), etc.

We have recently proposed to use the real-time change of muscle thickness detected using ultrasound, namely sonomyography (SMG), for the prosthetic control (Zheng et al. 2006) and the assessment of muscle fatigue (Shi et al. 2007), isometric muscle contraction (Shi et al. 2008), and dynamic muscle contraction (Huang et al. 2007; Guo et al. 2008). The real-time signal about the muscle thickness change during its contraction detected using A-mode ultrasound was named as one-dimensional sonomyography (1-D SMG). In this study, we compared the performances of 1-D SMG signal and surface EMG signal in tracking the waveforms being displayed during the guided movement of wrist extension in term of tracking accuracy. We hypothesized that 1-D SMG signal could better follow the guided waveforms, thus may have potential as a non-invasive method to detect skeletal muscle activities in vivo and to prosthetic control.

METHODS

A. Subjects

Sixteen healthy adults, including eight males (mean±SD age= 26.3±3.4 years; body weight = 70.3±11.9 kg; height =172.9 ± 8.5 cm) and eight females (mean±SD age =23.5 ± 1.2 years; body weight = 50.4 ± 4.1 kg; height = 160.3 ± 1.7 cm), volunteered to participate in this study and were tested within a period of two months. All the participants were right-hand-dominant without any known neuromuscular disorders. The human subject ethical approval was obtained from the relevant committee in the authors' institution and informed consents were obtained from all subjects prior to the experiment.

B. Data acquisition and processing

An ultrasound pulser/receiver (model 5052 UA, GE Panametrics, Inc. West Chester, OH, USA) was used to drive a 10 MHz single element ultrasound transducer (model V129, GE Panametrics, Inc., West Chester, OH, USA), and to amplify the received signals. The A-mode ultrasound signal was digitized by a high speed A/D converter card with a sampling rate of 200 MHz (Gage CS82G, Gage Applied Technologies, Inc, Canada). The surface EMG signal, captured from the EMG bipolar Ag-Agcl electrodes (Axon System, Inc., NY, USA), was amplified by a custom-designed EMG amplifier with a gain of 1000 and filtered by a 10-300 Hz band-pass analog filter within the amplifier, and then digitized by a data acquisition card (NI-DAQ 6024E, National Instruments Corporation, Austin, TX, USA) with a sampling rate of 4 KHz. The A-mode ultrasound signal was saved frame by frame together with surface EMG for subsequent analysis in a PC with 2.8 GHz Pentium IV microprocessor and 512 MB RAM. The frame rate of A-mode ultrasound was approximately 17 Hz, which was also applied to the data rates of SMG and EMG RMS signals.

The 10 MHz single element ultrasound transducer (radius 3 mm) was inserted into a custom-designed holder (radius 10 mm) made of silicone gel in order to attach the transducer to the skin stably (Fig. 4). The transducer together with the holder was positioned on the skin where the belly of extensor carpi radialis is. Double-sided adhesive tape was used to fixate the holder, while ultrasound gel was imposed between the transducer and skin. The EMG bipolar Ag-Agcl electrodes were attached to the skin surface near the ultrasound transducer and along the extensor carpi radialis muscle. The distance between the two electrodes was approximately 20 mm and an additional electrode for providing the reference electrical signal was placed near the head of ulna.

The A-mode ultrasound and surface EMG were collected, stored and analyzed by the software for ultrasound measurement of motion and elasticity (UMME, http://www.sonomyography.org) developed using Visual C++. The time delay between the two data collection systems was calibrated using a method similar to that described by

Huang et al. (2005, 2007). As the transducer moved cyclically up and down in a water tank, the two signals representing A-mode ultrasound, and simulated EMG respectively were collected and stored. The time delay between the data sets was calculated using a cross-correlation algorithm. The details can be found in our earlier study (Huang et al. 2007).

The muscle deformation signal, i.e. SMG, was extracted from the A-mode ultrasound. A cross-correlation algorithm was employed to track the displacements of upper and lower boundaries of extensor carpi radilis muscle during the wrist extension. The equation used to calculate the normalized one-dimensional cross-correlation is as follow:

$$R_{xy} = \frac{\sum_{i=0}^{N-1}[x(i)-\bar{X}][y(i)-\bar{Y}]}{\sqrt{\sum_{i=0}^{N-1}[x(i)-\bar{X}]^2 \sum_{j=0}^{N-1}[y[j]-\bar{Y}]^2}} \quad (1)$$

Where $\bar{X}$ and $\bar{Y}$ are the means of $x(i)$ and $y(j)$, respectively. It requires a referennce signal from an initial frame and would search for the signal most similar to the reference signal for estimating the object position in the updated frame. The A-mode ultrasound echoes reflected from the fat-muscle and muscle-bone interfaces were selected by two tracking windows (Fig. 2c) in the first frame. When the muscle was contracting, its dimensional changes induced the variations of distance between the interface of fat-muscle and that of muscle-bone, which would cause the A-mode ultrasound echoes to shift for a certain distance. The percentage deformation of the muscle is defined as

$$D = \frac{(d-d_0)}{d_0} \times 100\% \quad (2)$$

Where d_0 is the initial distance between the two echoes and d is the distance when the muscle is contracting.

The RMS amplitude of EMG was calculated and compared with the SMG signal to investigate which one could better follow the guiding waveforms during the wrist extension.

C. Experiment protocol

Before the experiment formally began, all the subjects were trained for two or three trials to make sure they were familiar with the experimental protocol. None of subject had been trained before. Both 1-D SMG and surface EMG signals were tested for their accuracy in following the displayed waveform patterns. As shown in Fig. 1, the subject was seated comfortably in an adjustable chair with his/her trunk fixed by a strap onto the back of the chair to prevent posture change during the test and the right forearm resting on the table with pronation. The elbow was flexed at approximately 140 degree between the upper arm and forearm. The angle between the upper arm and trunk was approximately 30 degrees. The subject was instructed to perform wrist extension under the guidance of displayed sinusoidal (Fig. 2a), square (Fig. 2d) and triangular waveforms (Fig. 2e) respectively. The order of the experiments was randomly selected for each subject. For the SMG test, the subject was required to perform several wrist extensions before each experiment in order to determine the amplitude of the muscle deformation signal extracted from A-mode ultrasound (i.e. 1-D SMG), and the amplitudes of the guiding waveforms were adjusted based on the obtained muscle deformation range. During the experiments, the subjects were encouraged to try their best to produce real-time muscle deformation signal, i.e. SMG, the same as the waveform being displayed on the screen by adjusting the range of their wrist movement in response to the visual feedback from the guiding waveforms. If the muscle deformation signal generated did not follow the guiding waveform well, the subjects could adjust the strength of their muscles in order to match the two waveforms better. The wrist extension rates were set to be 20, 30, 50 cycles per minute for each guiding waveform. Therefore, every subject totally performed nine tasks of wrist extension for the three different movement patterns (sinusoidal, square and triangular waveforms) for SMG tests (Fig. 2). Three repeated trials were performed for each task and there was a rest of 3 minutes between two adjacent trials to avoid muscle fatigue. The A-mode ultrasound signals were saved in the PC hard disk for further analysis. To make the system response time comparable to the subsequent EMG test, the EMG signals were also collected and analyzed during the ultrasound measurement but the EMG RMS signal was not displayed and the results not used.

The subjects were also instructed to perform another set of wrist extension tasks, using the RMS of their surface EMG signals to follow the reference waveforms. Similar testing protocol was adopted as that in the SMG test. To make the results comparable, during the EMG test, the A-mode ultrasound signals were collected and analyzed in real-time but the SMG signal was not displayed, as shown in Fig. 3. The subjects could adjust the range of wrist movement according to the real-time display of their EMG RMS signals to better fit the reference signal. Totally nine tasks of wrist extension for surface EMG test under the three wrist extension rates for the three different waveforms were performed by each subject. Figure 3 shows the interface of the software to collect the data of EMG RMS and the three types of guiding waveforms.

D. Data analysis

The SMG and EMG RMS data were respectively normalised by expressing measures as a percentage of the largest SMG and EMG RMS signals detected any time during the testing procedure. The RMS tracking errors (RMSTE) between SMG/EMG RMS and the corresponding guiding waveforms were calculated separately, defined as:

$$\text{RMSTE} = \sqrt{\frac{1}{N}\sum_{n=1}^{N}(Sig_1(n) - Sig_2(n))^2} \tag{3}$$

where $Sig_1(n), Sig_2(n)$ are signals with N points of values.

The performances of SMG and EMG RMS to follow the three guiding waveform patterns were compared using paired t-test. One-Way ANOVA was also used to determine whether there were any differences in the performances of the SMG signals under the three different movement rates. All the data were calculated using Minitab (Minitab Inc., Pennsylvania, USA). Statistical significance was set at the 5% probability level.

RESULTS

Totally 432 data sets were recorded from the sixteen subjects. Table 1 summarizes the RMS tracking errors of SMG and EMG for the three guiding waveform patterns under different movement rates. The overall mean RMS tracking errors of SMG under the three movement rates were 18.9±2.6% (mean± S.D.), 18.3±4.5%, and 17.0±3.4% for the sinusoid, square, and triangle guiding waveforms, while the corresponding values for EMG were 30.3±0.4 %, 29.0±2.7%, and 24.7±0.7 %, respectively (Fig. 5). Paired t-test revealed that the overall mean RMS tracking error of SMG was significantly smaller than that of EMG for all the three guiding waveforms.

One-way ANOVA showed that there were significant differences in the RMS tracking errors of SMG among the three wrist extension rates ($p<0.01$) for all the three guiding waveforms as demonstrated in Fig. 6. An apparent increasing trend of the RMS tracking error using SMG was observed with the increase of the movement rate for all the different guiding patterns. However, for EMG, statistical analysis revealed that the RMS tracking error was significantly different among the three movement rates only for the square waveform ($P=0.001$), but not for sinusoid ($P=0.921$) and triangle ($P=0.762$) waveforms. As shown in Fig. 7, the RMS tracking error for EMG generally showed smaller variations under different rates of wrist extension.

DISCUSSION

In this paper, we investigated the performances of surface EMG and 1D SMG, i.e. real-time muscle thickness change detected using A-mode ultrasound, in tracking three different movement patterns of the wrist extension guided by waveforms shown on the PC screen. We found that the tracking errors of SMG under different wrist extension rates (ranged from 14.0±1.9% to 23.3±3.7%) were statistically significantly smaller than the corresponding values of surface EMG (ranged from 24.2±4.4% to 32.1±4.1%) for all the movement patterns studied (Fig. 5 and Table 1), indicating that SMG performed better than surface EMG in following the given movement patterns in term of tracking accuracy.

For decades, EMG signal has been widely used in the areas of muscle fatigue (Masuda et al. 1998; Fukuda et al. 2006), muscle pathology (Haig et al. 1996; Hogrel 2005; Labarre et al. 2006; Ohata et al. 2006), prosthetic device control (Kermani et al. 1995; Boostani and Moradi 2003; Soares et al. 2003), and athlete muscle assessment under different postures (Worrell et al. 1992). Some researchers have demonstrated that the relationship between EMG and the force of the related joint was not linear (Alkner et al. 2000). Whereas, in our previous study, it was shown that the SMG signal was linear with the torque generated by biceps brachii muscles (Shi et al. 2008). These results may indicate that SMG signal may have a more direct, simple correlation (linear) with the torque generated by the corresponding muscle. The results of this study further demonstrate the potentials for SMG to serve as a feedback of rehabilitation of muscle dysfunction and assessment of muscle activity..

Compared with surface EMG, the main advantage of SMG is that ultrasound can inherently detect individual muscle at neighbouring locations and different depths without the effects of muscle cross talk by using one or more ultrasound transducers. Due to the challenges in separating SEMG signals generated by different neighbouring muscles, i.e. cross talk, the available prostheses controlled by SEMG could only provide limited number of DoFs. By using multi-channels of SMG signal, it is possible to realize the control of prostheses with multiple DoFs. It may benefit the users with more grasping functions and less training efforts.

Further studies are required to demonstrate these advantages quantitatively. It is also very interesting to further investigate whether the good performance of SMG on the extensor carpi radialis muscle for wrist control observed in this study can be applied to other skeletal muscles. A follow-up study using SMG to control real powered prostheses with a hand open-close feature is being conducted in our group. It has already been demonstrated that the muscles of residual limbs could generated SMG as well (Zheng et al. 2006).

It is interesting to explore why SMG could perform significantly better than EMG in tracking different given movement patterns of the joint under different movement rates. It has been reported that there is an exponential relationship between EMG magnitudes and the strengths generated by different skeletal muscles (Deluca 1997; Hodges et al. 2003; Zheng et al. 2006; Shi et al. 2008). We have previously found that SMG signals of a skeletal muscle have approximately linear relationships with the strengths generated by this muscle, represented either by torques for isometric contractions (Shi et al. 2008) or by joint angles for isotonic contractions (Zheng et al. 2006). It appears that SMG and the corresponding joint angle follow a relatively simple relationship in comparison with the relation between EMG and joint angle. The results of this and previous studies appear to imply that the architectural changes during muscle contraction relate more directly to the actuation achieved (mechanical output), while the EMG is a measure of activation intended (electrical input). In relation to the findings of the present study, we may interpret that our motor control and visual feedback system could perform better when the control signal has a linear relationship with the target signal to control, which is the wrist angle in this case. This may probably reduce the training efforts when the SMG signal is used for the prosthetic control. Further studies are required to study how many training efforts can be saved when using SMG for control instead of EMG. More normal and residual limbs should be tested to ensure a solid conclusion.

As expected, it was found that as the movement rates increased, the tracking errors of SMG increased (Fig. 6). When the movement rates increased, the subjects were required to perform the same movement in a shorter time period. Furthermore, according to subjects' verbal reports, the visual feedback used to provide instantaneous performance indication during the test slightly distracted their attention. Thus, as the movement rates increased, the possibility for SMG to "move away" from the guiding waveform may also increase, resulting in higher tracking errors. However, this increasing trend in tracking error with the increase of movement rate was not observed in EMG RMS (Fig. 7). It was also noted that the performance of SMG tracking at the highest rate was still better than the best performance of the EMG tracking among all the tests. The reducing performance of SMG induced by the increase of movement speed may have a number of potential reasons. First, the frame rate of A-mode ultrasound (approximately 17 Hz), which also determines how fast the data points of SMG signal are given, was relatively low in the study. With the increase of the wrist flexion-extension rate, the SMG data collected in each cycle would be reduced. Therefore, the subject may have fewer data points to refer to for following the given waveform. Since we have also controlled the data rate of EMG RMS to 17 Hz during the test, this effect should have affected the performance of EMG tracking as well when the movement speed was increased, however, it was not observed in this study. A higher frame rate system could be used to further investigate the effect of data collection speed in future studies. The second possible reason is that SMG is a signal not only related to the bioelectrical properties of muscles, i.e. how muscles are activated, but also dependent on the mechanical properties of muscle-tendon complex, i.e. viscoelastic properties. With the increase of the muscle contraction speed, the hysteresis of SMG signal may also increase. This will make it more challenging for the subjects to follow the given movement patterns using SMG signal. However, EMG signals would not be affected by this effect, as they are more related to bioelectrical properties of muscles. Again, further studies are required to better understand the effects of the viscoelasticity of muscles and other tissues on the generation and applications of SMG signal.

In summary, we demonstrated in this study that SMG signal obtained using A-mode ultrasound could provide better performance flexion-extension of wrist in comparison with EMG in tracking different given patterns under different wrist flexion-extension rates. The use of single element transducer in A-mode image allowed great flexibility in designing SMG sensor, thus it is practically feasible to attach such a probe on the skin surface conveniently for the purposes of control or muscle function evaluation, similar to the use of surface EMG. However, further studies are required to verify the performances of SMG signals on different muscles under different conditions. The mechanism of how the increasing movement rate of wrist affects the SMG tracking performances should also be further investigated.

ACKNOWLEDGMENTS

This work was supported by The Hong Kong Polytechnic University (G-YE22, 1-BB69) and the Grant Council of Hong Kong (PolyU 5331/06E).

REFERENCES

Abboudi RL, Glass CA, Newby NA, Flint JA, Craelius W. A biomimetic controller for a multifinger prosthesis. IEEE T Rehabil Eng 1999;7:121–129.

Alemu M, Kumar DK, and Bradley A. Time-frequency analysis of SEMG - with special consideration to the interelectrode spacing. IEEE Trans Neural Syst Rehabil Eng 2003;11:341-345.

Alkner BA, Tesch PA, Berg HE. Quadriceps EMG/force relationship in knee extension and leg press. Med Sci Sports Exerc 2000; 32:459-63.

Almstrom C, Kadefors R. Methods for transducing skin movements in the control of assistive devices. In: Proceedings of Third International Conference on Medical Physics. 1972. vol. 33. Sweden pp. 2.

Balogh I, Hansson GA, Ohlsson K, Stromberg U, Skerfving S. Interindividual variation of physical load in a work task. Scand J Work Env Hea 1999;25:57-66.

Bolton CF, Parkers A, Thompson TR, Clark MR, Sterne CJ. Recording sound from human skeletal muscle: technical and physiological aspects. Muscle Nerve 1989;12: 126-134.

Boostani R, Moradi MH. Evaluation of the forearm EMG signal features for the control of a prosthetic hand. Physiol Meas 2003;24:309-319.

Curcie DJ, Flint JA Craelius W. Biomimetic finger control by filtering of distributed forelimb pressures. IEEE Trans Neural Syst Rehabil Eng 2001;9:69-75.

De Luca CJ. The use of surface electromyography in biomechanics. J Appl Biomech 1997;13:135-163.

De Luca CJ. Surface electromyography: detection and recording. Boston: DelSys Inc, 2002.

Fukuda K, Umezu Y, Shiba N, Tajima F, Nagata K. Electromyographic fatigue analysis of back muscles during remote muscle contraction. J Back Musculoskelet 2006;19:61-66.

Fukunaga T, Kubo K, and Kawakami Y. In vivo behaviour of human muscle tendon during walking. Proc Biol Sci 2001; 268:229-233.

Georgiakaki I, Tortopidis D, Garefis P, Kiliaridis S. Ultrasonographic thickness and electromyographic activity of masseter muscle of human females. J Oral Rehabil 2007; 34:121-128.

Guo JY, Zheng YP, Huang QH, Chen X. Dynamic Monitoring of Forearm Muscles Using 1D Sonomyography (SMG) System. J Rehabil Res Dev 2008; 45: 187-196.

Haig AJ, Gelblum JB, Rechtien JJ, Gitter AJ. Technology assessment: the use of surface EMG in the diagnosis and treatment of nerve and muscle disorders. Muscle Nerve 1996;19:392-395.

Heasman JM, Scott TRD, Kirkup L, Flynn RY, Vare VA Gschwind CR. Control of a hand grasp neuoprosthesis using an electroencephalogram-triggered switch: demonstration of improvements in performance using wavepacket analysis. Med Biol Eng Comput 2002; 40:588–593.

Hodges PW, Pengel LHM, Herbert RD, Gandevia SC. Measurement of muscle contraction with ultrasound imaging. Muscle Nerve 2003;27:682-692.

Hogrel JY. Clinical applications of surface electromyography in neuromuscular disorders. Neurophysiol Clin 2005;35:59-71.

Huang QH, Zheng YP, Lu MH, and Chi ZR. Development of a portable 3D ultrasound imaging system for musculoskeletal tissues. Ultrasonics 2005; 43:153-163.

Huang QH, Zheng YP, Chen X, He JF, Shi J. Synchronization between somyography, electromyography and joint angle. Open Biomed Eng J 2007;1:77-84.

Karlsson S, Gerdle B. Mean frequency and signal amplitude of the surface EMG of the quadriceps muscles increase with increasing torque- a study using the continuous wavelet transform. J Electromyogr Kinesiol 2001;11:131-140.

Kenney LP, Lisitsa I, Bowker P, Heath GH, Howard D. Dimensional change in muscle as a control signal for powered upper limb prostheses: a pilot study. Med Eng Phys 1999;21:589-597.

Kermani MZ, Wheeler BC, Badie K, Hashemi TM. EMG feature evaluation for movement control of upper extremity prostheses. IEEE Trans Rehabil Eng 1995;3:324-333.

Labarre VA.Assessment of muscle function in pathology with surface electrode EMG. Rev Neurolvol 2006;162:459-465.

Lieber RL, Friden J. Functional and clinical significance of skeletal muscle architecture. Muscle Nerve 2000;23:1647-1666.

Mademli L, Arampatzis A. Behaviour of the human gastrocnemius muscle architecture during submaximal isometric fatigue. Eur J Appl Physiol 2005;94:611-617.

Maganaris CN. Force-length characteristics of in vivo human skeletal muscle. Acta Physiol Scand 2001;172:279-285.

Mahlfeld K, Franke J, Awiszus F. Postcontraction changes of muscle architecture in human quadriceps muscle. Muscle Nerve 2004;29:597-600.

Masuda K, Masuda T, Sadoyama T, Inaki M, Katsuta S. Changes in surface EMG parameters during static and dynamic fatiguing contractions. J Electromyogr Kinesiol 1998; 9:39-46.

McMeeken JM, Beith ID, Newham DJ, Milligan P, Critchley DJ. The relationship between EMG and change in thickness of transversus abdominis. Clin Biomech 2004;19:337-342.

Nicolelis MAL. Actions from thoughts. Nature 2001;409:403–407.

Ohata K, Tsuboyama T, Ichihashi N, Minami S. Measurement of muscle thickness as quantitative muscle evaluation for adults with severe cerebral palsy. Phys Ther 2006;86:1231-1239.

Orizio C. Muscle sound: bases for the introduction of a mechnomoygraphic signal in muscle studies. Crit Rev Biomed Eng 1993; 21:201–243.

Oster G. Muscle sound. Sci Am 1984;250:108–114.

Reeves ND, Maganaris CN, Narici MV. Ultrasonographic assessment of human skeletal muscle size. Eur J Appl Physiol. 2004; 91:116-118.

Sallinen J, Ojanen T, Karavirta L, Ahtiainen JP, Hakkinen K. Muscle mass and strength, body composition and dietary intake in master strength athletes vs untrained men of different ages. J Sports Med Phys Fitness. 2008; 48:190-196.

Shi J, Zheng YP, Chen X, Huang QH. Assessment of muscle fatigue using sonomyography: Muscle thickness change detected from ultrasound images. Med Eng Phys 2007;29:472-479.

Shi J, Zheng YP, Huang QH, Chen X. Relationships among continuous sonomyography, electromyography and torque generated by normal upper arm muscles during isometric contraction. IEEE T Bio-Med Eng 2008; 55:1191-1198.

Soares A, Andrade A, Lamounier E, Carrijo R. The development of a virtual Myoelectric prosthesis controlled by an EMG pattern recognition system based on neural networks. J Intell Inf Syst 2003;21:127-141.

Taylor DM, Tillery SIH, Schwartz AB. Direct cortical control of 3D neuroprosthetic device. Science 2002;296:1829–1832.

Whittaker J, Teyhen D, Elliott J, Cook K, Langevin H, Dahl H, Stokes M. Rehabilitative Ultrasound Imaging: Understanding the Technology and its Applications. J Orthop Sports Phys Ther 2007;37: 435-449.

Worrell TW, Corey BJ, York SL, Santiestaban J. An analysis of supraspinatus EMG activity and shoulder isometric force development. Med Sci Sport Exer 1992;24:744-748.

Zecca M, Micera S, Carrozza MC. Control of multifunctional prosthetic hands by processing the electromyographic signal. Crit Rev Biomed Eng 2002;30:459-485.

Zheng YP, Chan MM, Shi J, Chen X, Huang QH. Sonomyography: Monitoring morphological changes of forearm muscles in actions with the feasibility for the control of powered prosthesis. Med Eng Phys 2006;28:405-415.

Zwarts MJ, Stegeman DF. Multichannel surface EMG: basic aspects and clinical utility. Muscle Nerve 2003;28:1 – 17.

Captions of Figures

Fig. 1 The diagram of the data collection system.

Fig. 2 The software interface was used to simultaneously collect 1-D SMG, SEMG signals (a) The sinusoidal waveform with a rate of 20 cycles per minute was used to guide the wrist extension movement. The subject used 1-D SMG signal to track the sinusoidal pattern. (b) Surface EMG was also collected for reference. (c) The muscle deformation signal (i.e. SMG) was measured by detecting the distance change between the A-mode ultrasound echoes reflected from the fat-muscle and muscle-bone interfaces, which were selected by two the tracking windows. A cross-correlation algorithm was employed to track the movements of the echoes during the wrist extension. The muscle deformation signal (i.e. SMG) was calculated using the change of the time interval between the echoes and displayed along with the guiding waveform for tracking (a). (d) 1-D SMG signal tracks the square waveform with a rate of 30 cycles per minute; (e) 1-D SMG signal tracks the triangular waveform with a rate of 50 cycles per minute.

Fig. 3 (a) The software interface was used to collect the SEMG and A-mode ultrasound signals. (a) SEMG signal was collected. (b) The sinusoidal waveform with a rate of 20 cycles per minute was used to guide the wrist extension movement. SEMG RMS was calculated to track the sinusoidal pattern. (c) A-mode ultrasound signal was also collected for reference (d) SEMG RMS tracks the square waveform with a rate of 30 cycles per minute; (e) SEMG RMS tracks the triangular waveform with a rate of 50 cycles per minute.

Fig. 4 Placement of the 1D ultrasound transducer, SEMG electrodes on the forearm, with ultrasound gel applied between the ultrasound transducer and skin to aid acoustic coupling.

Fig. 5 The RMS tracking errors (%) between SMG/SEMG and the guiding waveforms. The error bar represents the standard deviation of the results of three different movement rates.

Fig. 6 The tracking errors of SMG for the three guiding waveforms under different movement rates. The error bar represents the standard deviation of the results of the sixteen subjects.

Fig. 7 The RMS tracking errors of SEMG under the three different wrist extension rates for different guiding waveforms. The error bar represents the standard deviation of the results of the sixteen different subjects.

Table 1. The RMS tracking errors (%) between SMG/surface EMG and the guiding waveforms at the three movement rates (Mean ± S.D.) and the mean RMS tracking errors averaged over the three movement rates for sinusoid, square, and triangle guiding waveforms.

Rate (Cycles per minute)	*SMG*			*Surface EMG*		
	sinusoid	*square*	*triangle*	*sinusoid*	*square*	*triangle*
20	16.3±7.8	14.6±1.7	14.0±1.9	30.5±4.7	27.0±4.2	24.2±4.4
30	19.0±3.0	17.1±1.6	16.3±2.5	29.9±6.4	27.8±3.0	24.4±6.3
50	21.5±3.2	23.3±3.7	20.7±3.1	30.6±5.5	32.1±4.1	25.4±4.8
Mean	18.9±2.6	18.3±4.5	17.0±3.4	30.3±0.4	29.0±2.7	24.7±0.7

Figure 1

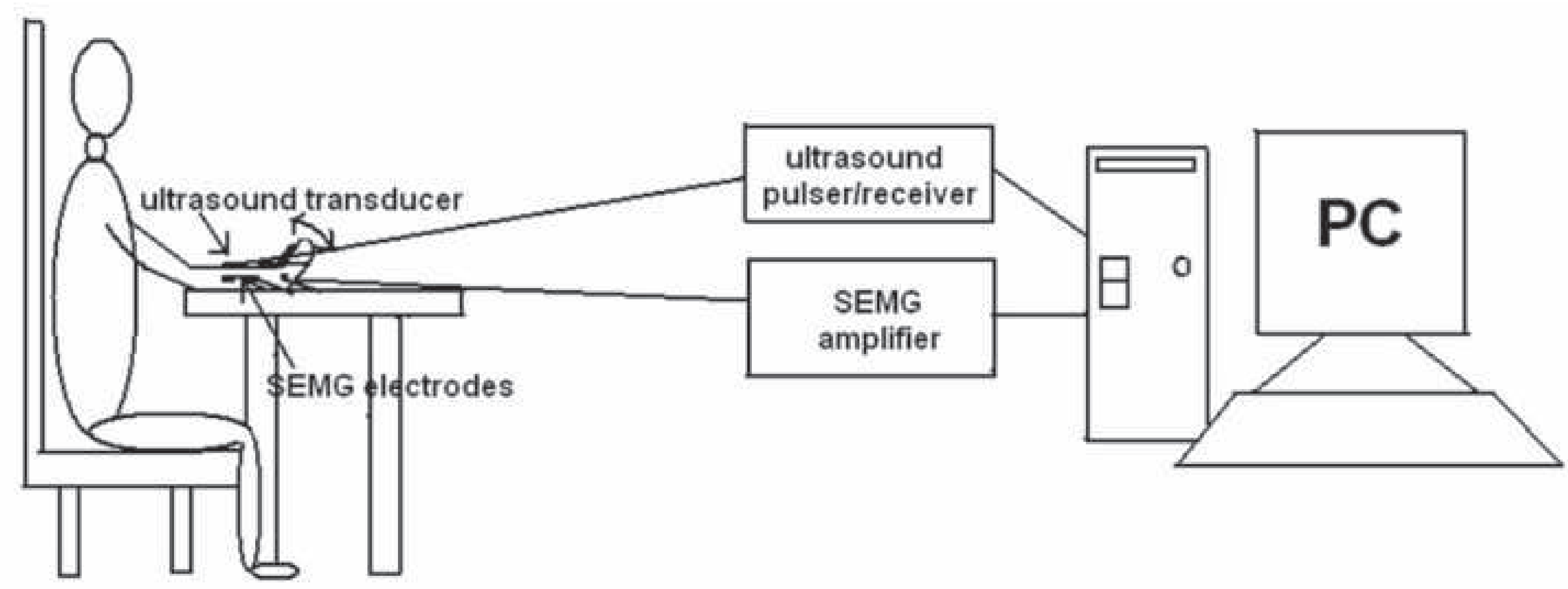

Fig. 1

Figure 2

Click here to download high resolution image

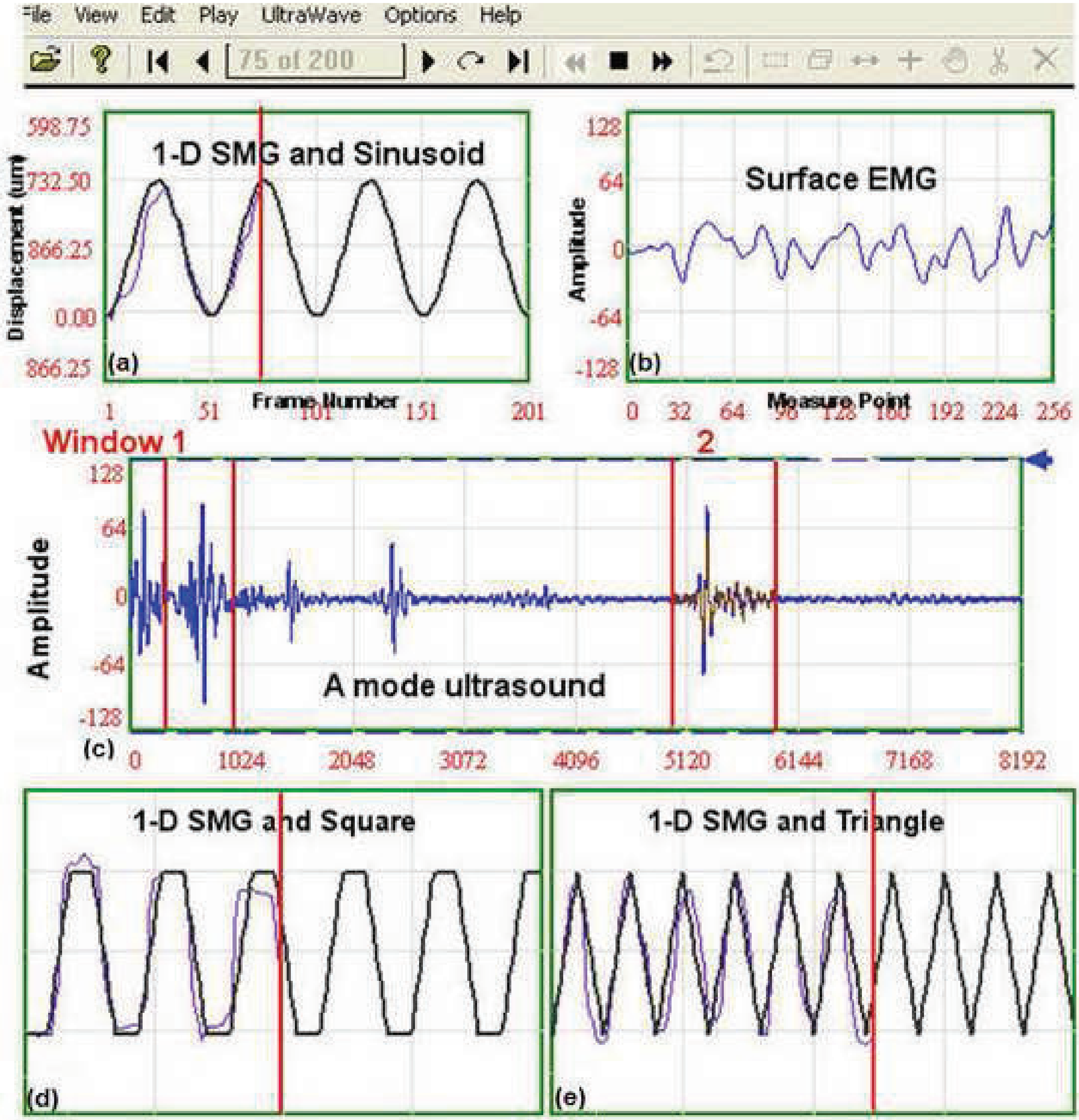

Fig. 2

Figure 3
Click here to download high resolution image

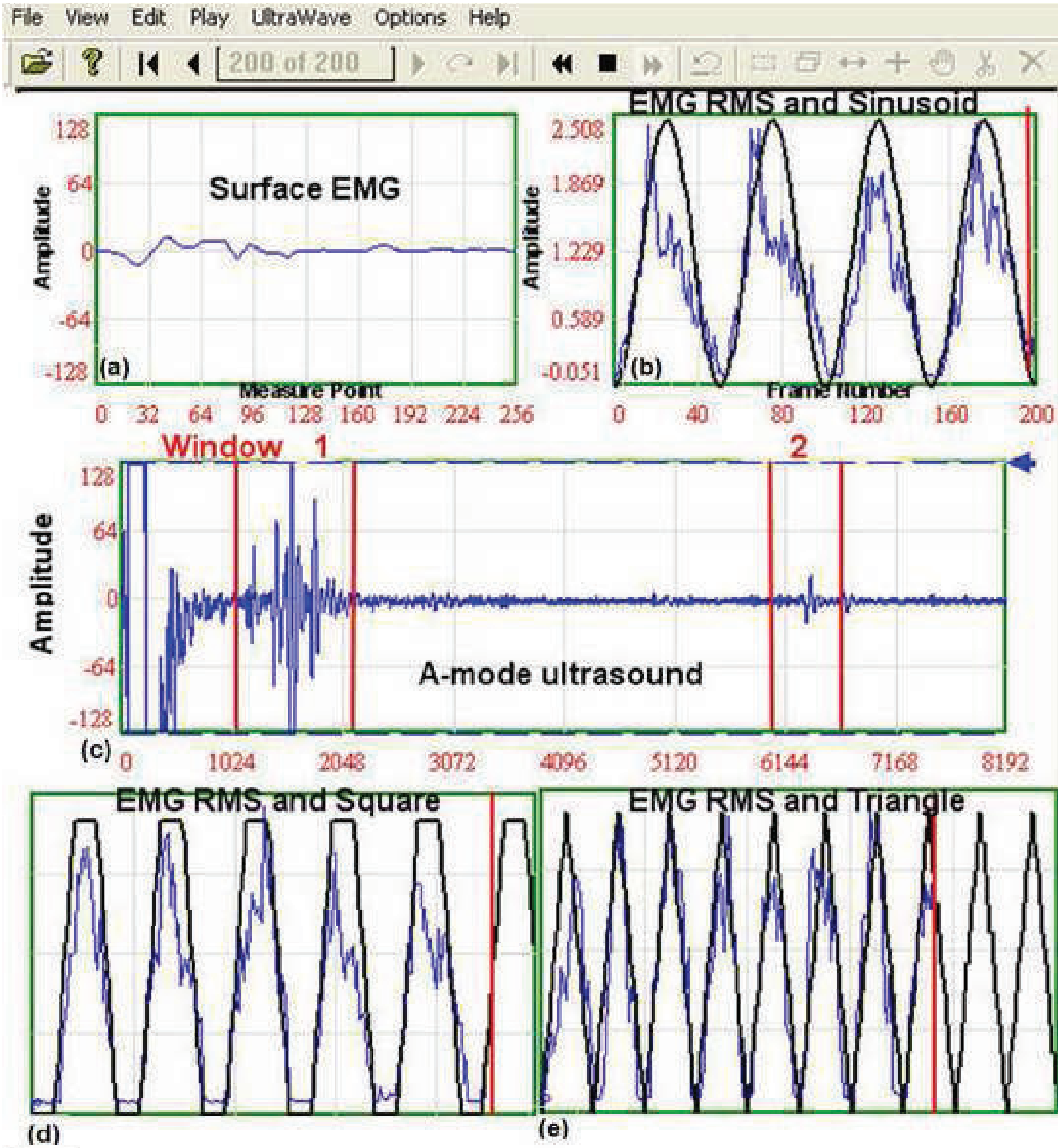

Fig. 3

Figure 4

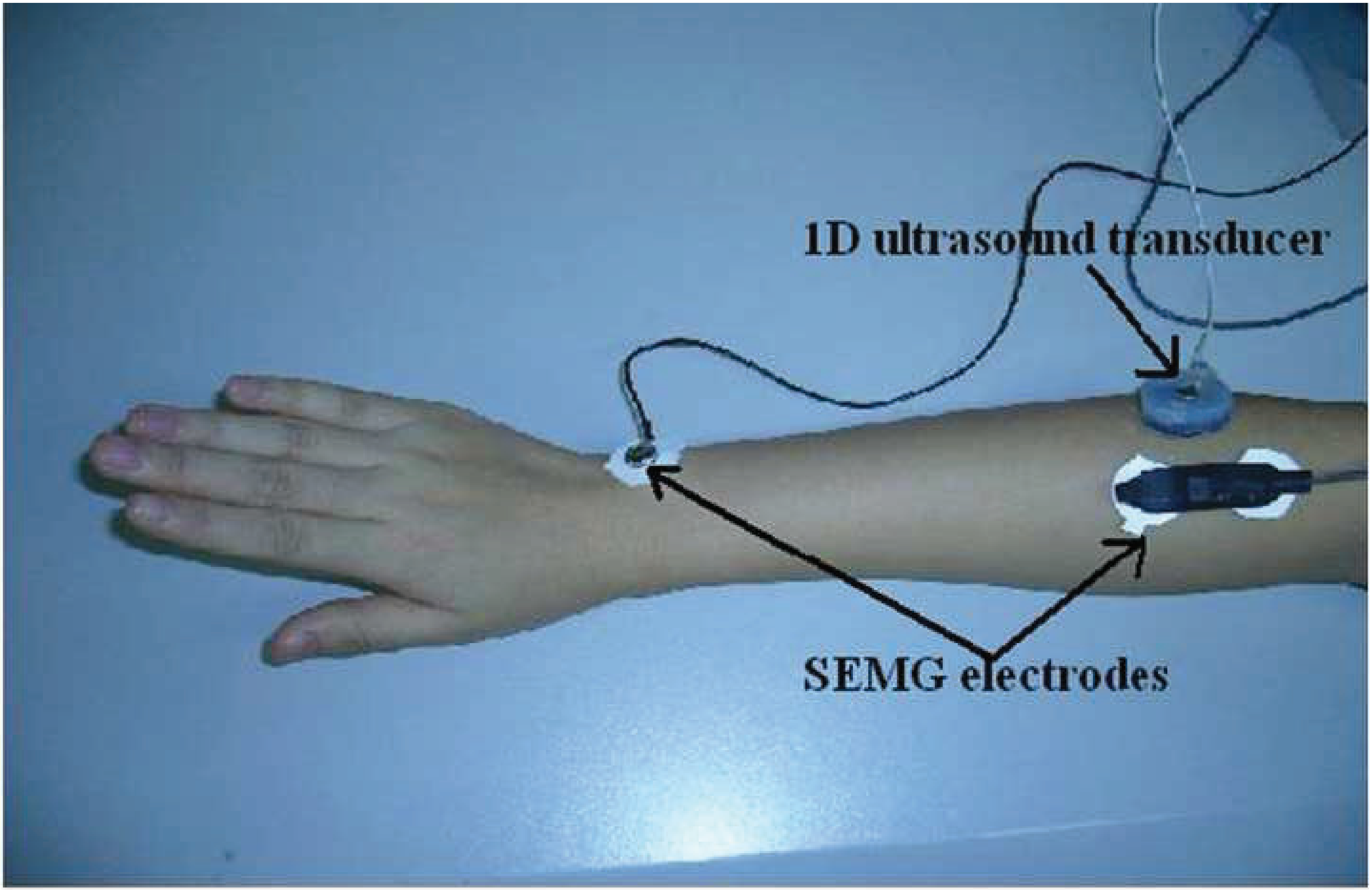

Fig. 4

Figure 5

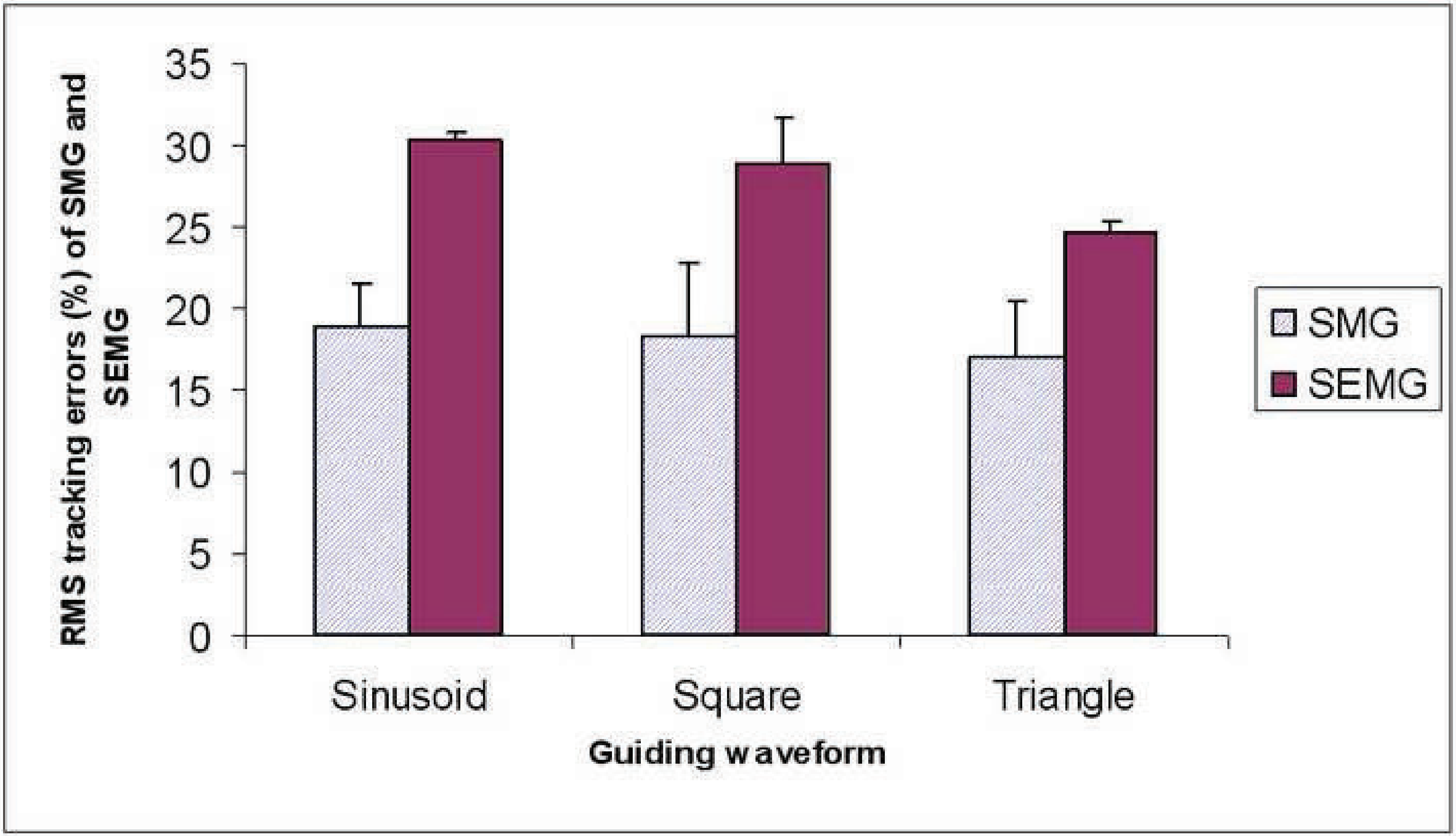

Fig. 5

Figure 6

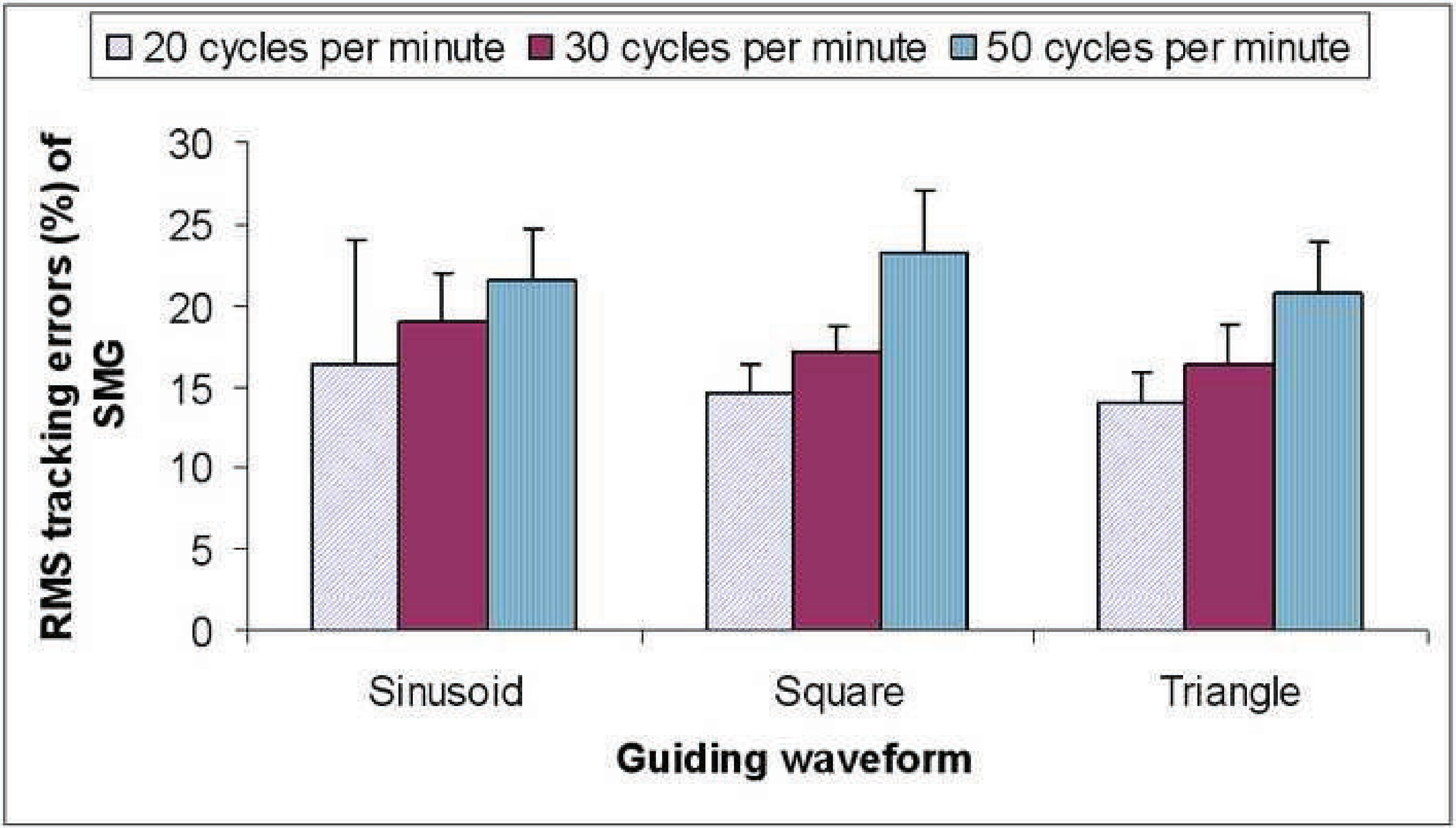

Fig. 6

Figure 7

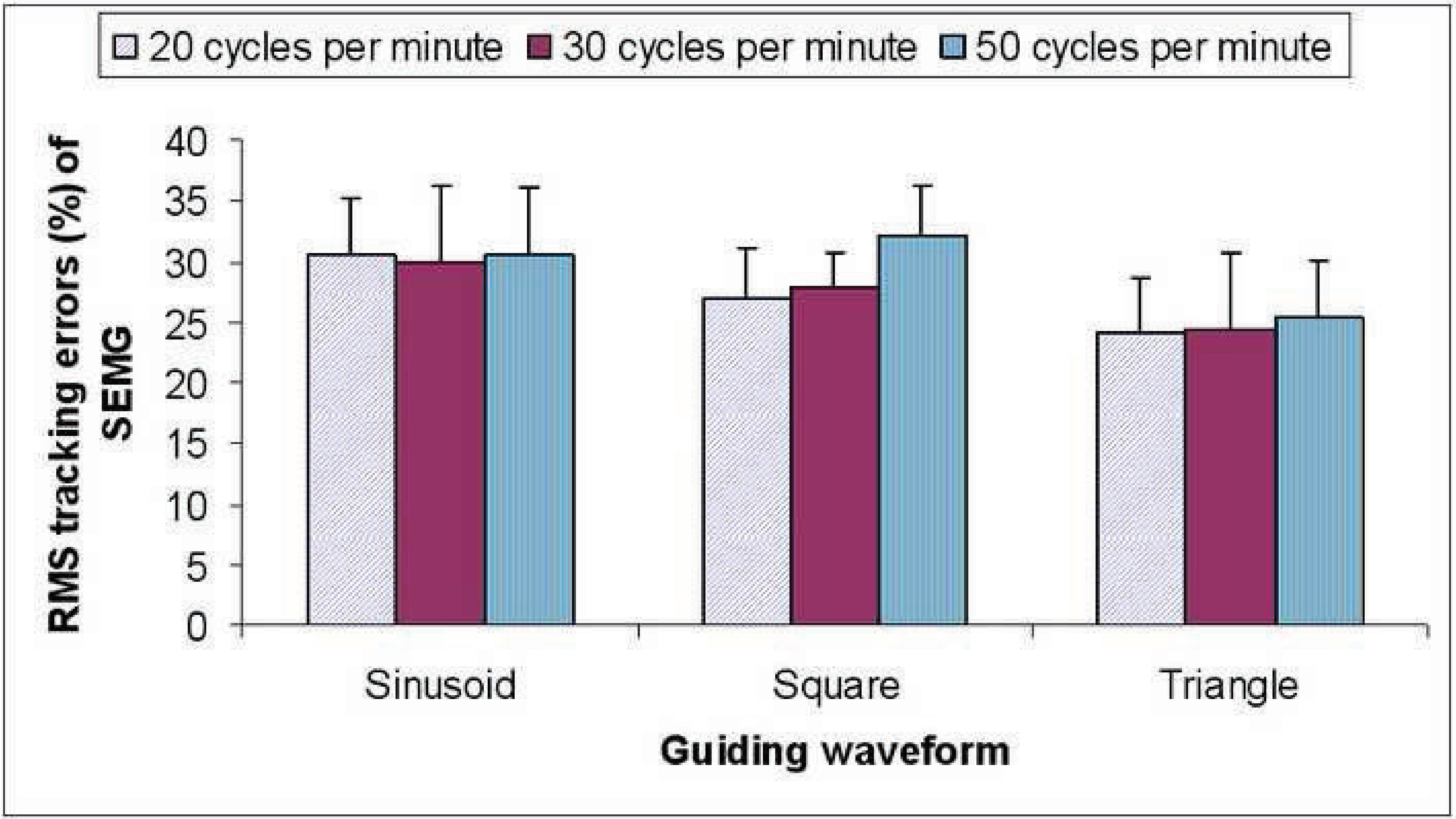

Fig. 7